Editors' Suggestion

Observation of Hopping and Blockade of Bosons in a Trapped Ion Spin Chain

S. Debnath,[1,*] N. M. Linke,[1] S.-T. Wang,[2] C. Figgatt,[1] K. A. Landsman,[1] L.-M. Duan,[2] and C. Monroe[1]
[1]Joint Quantum Institute, Department of Physics, and Joint Center for Quantum Information and Computer Science, University of Maryland, College Park, Maryland 20742, USA
[2]Department of Physics, University of Michigan, Ann Arbor, Michigan 48109, USA

(Received 8 November 2017; published 12 February 2018)

The local phonon modes in a Coulomb crystal of trapped ions can represent a Hubbard system of coupled bosons. We selectively prepare single excitations at each site and observe free hopping of a boson between sites, mediated by the long-range Coulomb interaction between ions. We then implement phonon blockades on targeted sites by driving a Jaynes-Cummings interaction on individually addressed ions to couple their internal spin to the local phonon mode. The resulting dressed states have energy splittings that can be tuned to suppress phonon hopping into the site. This new experimental approach opens up the possibility of realizing large-scale Hubbard systems from the bottom up with tunable interactions at the single-site level.

DOI: 10.1103/PhysRevLett.120.073001

Trapped atomic ions are an excellent medium for quantum computation and quantum simulation, acting as a many-body system of spins with programmable and reconfigurable Ising couplings [1–3]. In this system, the long-range spin-spin interaction is mediated by the collective motion of an ion chain and emerges over time scales longer than the propagation time of mechanical waves or phonons through the crystal [4,5]. On the other hand, at shorter time scales, such a chain represents a bosonic system of phonon modes that describe the local motion of individual ions. Here each local mode is defined by the harmonic confinement of a particular ion with all other ions pinned. In this picture, phonons hop between the local modes due to the long-range Coulomb interaction between ions [6–8]. This intrinsic hopping in trapped ion crystals makes it a viable candidate for simulating many-body systems of bosons [6,7], boson interference [9], and applications such as boson sampling [10].

Such a system of local oscillators can be approximated to the lowest order of the transverse ion displacement by the phonon Hamiltonian ($\hbar = 1$):

$$H_p = \sum_j (\omega_x + \omega_j) a_j^\dagger a_j + \sum_{j<k} \kappa_{jk} (a_j^\dagger a_k + a_j a_k^\dagger). \quad (1)$$

Here the local mode frequency of each ion is expressed as a sum of the common mode transverse trap frequency ω_x and a position-dependent frequency shift ω_j experienced by the jth ion [6,7]. The local mode bosonic creation and annihilation operators are $a_j^\dagger$ and a_j, respectively. The long-range hopping term $\kappa_{jk} = e^2/(2M\omega_x d_{jk}^3)$ is determined by the distance d_{jk} between ions j and k, where e and M are the charge and mass, respectively, of a single ion.

By applying external controls to the system, on-site interactions between phonons lead to the simulation of Hubbard models of bosons. For instance, applied position-dependent Stark shifts can result in effective phonon-phonon interactions [6]. Combined with phonon hopping between sites, such a system follows the Bose-Hubbard model. In the approach considered here, the internal spin is coupled to the external phonon mode by driving the spin resonance on a motion-induced sideband transition [11]. This gives rise to nonlinear on-site interactions between spin-phonon excitations (polaritons). Such a system simulates the Jaynes-Cummings-Hubbard model, which describes an array of coupled cavities [7,8,12–14].

In order to study the dynamics of such bosonic systems, the local phonon modes must be manipulated and detected faster than the hopping rate. Addressing these modes requires fields that target individual ions in space and each local mode in frequency. Previous experiments have observed hopping only between two sites either by using the collective motion of ions in separate but nearby trapping zones [15,16] or by varying the spacing between ions in the same trap to spatially resolve each site [17]. In contrast, the direct addressing of each local mode in a single-ion crystal circumvents such overheads and provides a complete toolbox for implementing larger bosonic systems by simply increasing the number of ions.

In this Letter, we report the observation of free phonon hopping in an ion chain and study its suppression by applying targeted phonon blockades on individual sites. We access all local motional modes along the transverse direction of a static linear chain of $^{171}Yb^+$ ions. Phonons are prepared and measured by driving sideband transitions on each mode faster than the rate of hopping in the chain, with an overall fidelity of 89(2)%. This is achieved by

setting the transverse confinement to be much larger than the axial confinement of the chain, which results in suitably low hopping rates due to both a relatively large interion distance ($\sim 10\ \mu$m) and high mass of the $^{171}Yb^{+}$ ion.

A phonon blockade is implemented by resonantly driving red-sideband transitions on each site, which couple the internal spin of individually addressed ions to their local phonon mode via a Jaynes-Cummings interaction. In the rotating frame of the free spin and the transverse motional common-mode Hamiltonian ($H_0 = \omega_{HF}\sum_j |e\rangle_j\langle e|_j + \omega_x \sum_j a_j^\dagger a_j$), this interaction is represented by the blockade Hamiltonian as

$$H_b = \sum_j \Delta_j |e\rangle_j\langle e|_j + \sum_j \frac{\Omega_j^r}{2}(\sigma_j^+ a_j + \sigma_j^- a_j^\dagger). \quad (2)$$

Here, the spin-1/2 "ground" and "excited" states of the jth ion are represented by $|g\rangle_j$ and $|e\rangle_j$, respectively, with energy splitting ω_{HF} and spin raising and lowering operators σ_j^+ and σ_j^-, respectively. A local motional red sideband is driven at a Rabi frequency Ω_j^r and detuned from resonance by Δ_j.

Phonon blockades are applied on individual sites that have ions prepared in the ground state of spin and motion $|g,0\rangle$, where the second index denotes the local mode phonon number. Upon applying the Jaynes-Cummings interaction at resonance ($\Delta_j = 0$), a maximal energy splitting of $|\omega_j \pm \Omega_j^r/2|$ occurs between $|g,0\rangle$ and the next excited polaritonic states $|\pm,1\rangle$. This energy cost suppresses phonons from entering the targeted sites and thereby creates a blockade [see Fig. 1(a)]. This scheme is analogous to implementing photon blockades using single-atom cavity QED systems [18].

The experiment consists of a linear chain of three $^{171}Yb^{+}$ ions, each with an internal spin defined by a pair of hyperfine "clock" states as $|g\rangle = |F=0, m_F=0\rangle$ and $|e\rangle = |F=1, m_F=0\rangle$ of the $2S_{1/2}$ electronic ground level with a hyperfine energy splitting of $\omega_{HF} = 2\pi \times 12.642812$ GHz [19]. Here, F and m_F denote the quantum numbers associated with the total atomic angular momentum and its projection along the quantization axis defined by an applied magnetic field of 5.2G, respectively. The external motion of the trapped ions is defined by a linear rf-Paul trap with transverse (X,Y) and axial (Z) harmonic confinement at frequencies $\{\omega_x,\omega_y,\omega_z\} = 2\pi \times \{3.10, 2.85, 0.15\}$ MHz such that the ion chain is aligned along Z with a distance of $d_{j,j+1} = 10.1(2)\ \mu$m between adjacent ions. During an experiment, we excite local phonons in the transverse modes along X, which can then hop between the ion sites. The inherent hopping rates are approximately $\kappa_{j,j+1} \approx 2\pi \times 3$ kHz and $\kappa_{j,j+2} \approx \kappa_{j,j+1}/8$, respectively. The combined effect of the transverse (X) harmonic confinement and repulsion between ions (determined by d_{jk}) defines the position-dependent local mode frequency shifts $\{\omega_j\}$. Figure 1(a) represents the local modes with frequencies $\{\omega_j\}$ in a frame rotating at the common mode frequency ω_x.

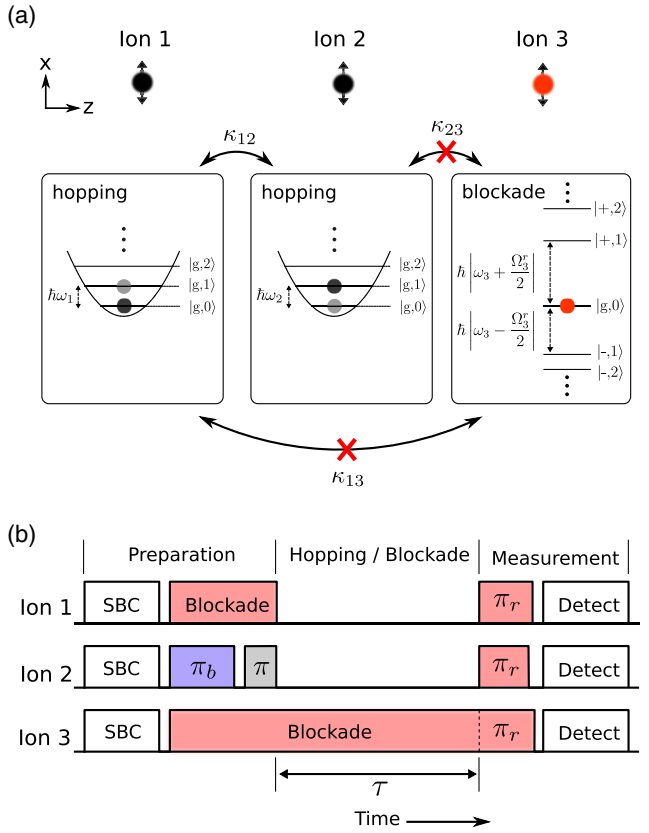

FIG. 1. Experimental system for observing the hopping of a single phonon excitation between local transverse motional modes along the X direction. (a) The local phonon frequencies are represented by ω_j in a frame rotating at the transverse common mode frequency ω_x, and κ_{jk} is the phonon hopping strength between modes j and k. Phonon blockades on individual sites (here ion 3) is implemented by driving resonant red-sideband transitions with strength Ω_j^r that gives rise to an energy splitting between the ground state $|g,0\rangle$ and the first excited polaritonic states $|\pm,1\rangle$. (b) An experimental sequence where each ion is prepared in the ground state of spin and motion $|g,0\rangle$ using Raman sideband cooling (SBC). A single phonon is excited on ion 2 using π pulses at the blue-sideband (π_b) and carrier (π) transitions. Local phonon blockades are applied using resonant red-sideband pulses (shown in red). The hopping duration τ is varied to observe the dynamics of local phonon occupancy (0 or 1 phonon) measured by first projecting it to the internal spin states ($|g\rangle$ or $|e\rangle$) of each ion using red-sideband π pulses (π_r) followed by the detection of state-dependent fluorescence from each ion using a photomultiplier tube array.

Coherent control of the spin and motion of each ion is implemented with stimulated Raman transitions using a 355 nm mode-locked laser [20], where pairs of Raman beams couple the spin of an ion to its transverse motion [3]. A global beam illuminates the entire chain, and a counter-propagating array of individual addressing beams is focused to a waist of $\approx 1\ \mu$m at each ion. The beat note

between the Raman beams can then be tuned to ω_{HF} to implement a "carrier" transition for coherent spin flips or tuned to $\omega_{HF} \pm (\omega_x + \omega_j)$ to drive a blue- or red-sideband transition involving local phonon modes. The individual addressing beams are modulated independently using a multichannel acousto-optic modulator [21], each channel of which is driven by a separate arbitrary waveform generator [22]. The wave vector difference $\Delta\vec{k}$ between Raman beams has a projection along both the X and Y directions of motion. Each transverse mode can then be addressed by tuning near their sideband transitions. In order to spectrally resolve each local mode, we choose sideband Rabi frequencies $\Omega_j^r, \Omega_j^b < |\omega_x - \omega_y|$ while also satisfying $|\omega_j| \ll |\omega_x - \omega_y|$ to prevent cross talk between the modes.

A typical experimental sequence, as shown in Fig. 1(b), starts with the preparation of each ion in state $|g, 0\rangle$ by Doppler cooling and subsequent Raman sideband cooling of each of the transverse modes. A single-phonon excitation is introduced at a single site by resonantly driving a blue-sideband and carrier π pulse to prepare the state $|g, 1\rangle$. In order to minimize the effect of hopping during this process, the sideband and carrier π pulses are kept short ($\approx$10 and $\approx$1 μs, respectively). Phonon blockades are applied to particular ions, initially prepared in the $|g, 0\rangle$ state, by resonantly driving the red sidebands of their respective local modes. Finally, the single-phonon occupancy denoted by states $|g, 0\rangle$ and $|g, 1\rangle$ is measured at each site using a red-sideband π pulse on each ion, which coherently projects it to spin states $|g\rangle$ and $|e\rangle$, respectively. The spin-dependent fluorescence can then be detected using a multichannel photomultiplier tube, thereby measuring a binary phonon occupancy of 0 or 1 for each site [3,19].

Figure 2 shows the hopping dynamics. During free hopping, a single excitation is observed to hop predominantly to the neighboring site. The extent of hopping is indicated by the amplitude of the oscillations in phonon occupancy. This is determined by the strength of hopping κ_{jk} relative to the energy splitting between local modes $\omega_{jk} = \omega_j - \omega_k$. We observe different hopping rates between ions 1 and 2 compared to that between 2 and 3, which indicates an asymmetry in the local mode energy differences, $|\omega_{12}| \neq |\omega_{23}|$. This is likely due to a stable nonlinearity in the transverse confinement of the ion trap. We also note that the sign of the local mode energy difference is critical in governing next-nearest-neighbor hopping in systems with three or more modes. This is due to a Raman-type hopping process where appropriate energy splittings between the local modes can facilitate hopping between ion 1 and 3 via ion 2 (see Supplemental Material [23]).

Phonon hopping is also observed in the presence of a blockade applied on neighboring sites [Figs. 2(d)–2(g)]. Here, we resonantly drive on the red sideband, creating a ladder of Jaynes-Cummings eigenstates $\{|g, 0\rangle, |\pm, 1\rangle, |\pm, 2\rangle, \ldots\}$, where $|\pm, n\rangle$ is a spin-phonon dressed state with polaritonic excitation number n [Fig. 1(a)]. Since the blockade ion is initially in eigenstate $|g, 0\rangle$, hopping into

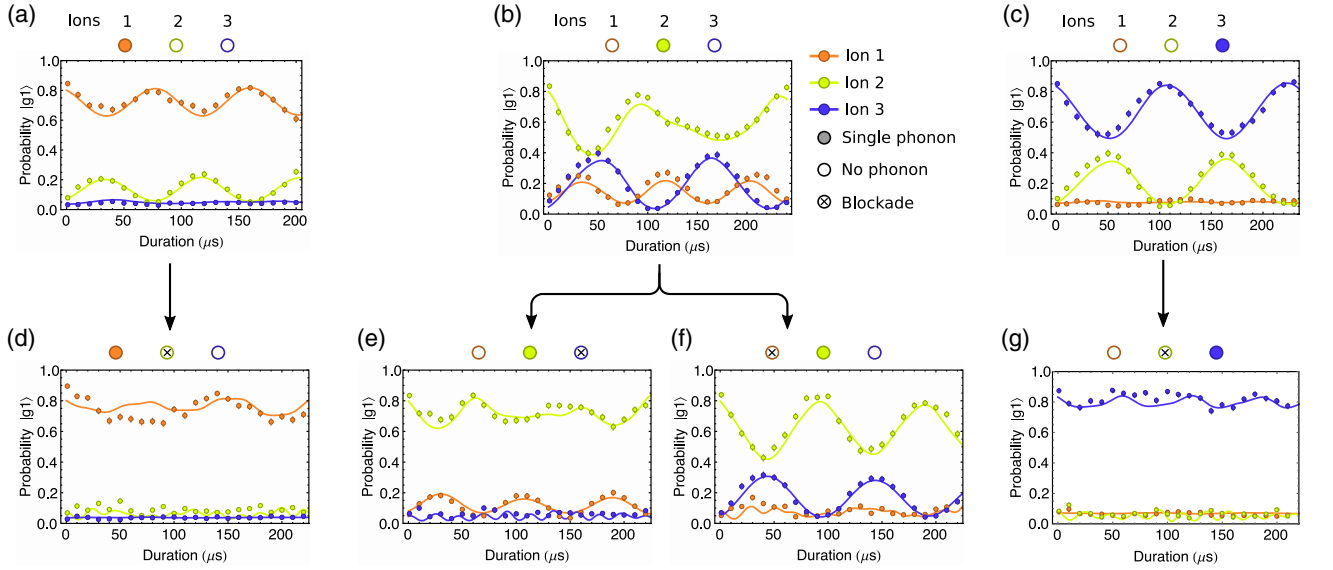

FIG. 2. The evolution of local phonon occupancies with initial single-phonon excitations on ions 1, 2, and 3 as shown by the shaded orange, green, and blue circles, respectively. In the absence of a blockade [(a)–(c)], the dynamics are governed by the hopping strengths $\{\kappa_{jk}\}$ and the local mode frequencies $\{\omega_j\}$. The corresponding dynamics in the presence of a blockade [(d)–(g)] indicate hopping suppression, which is determined by the blockade strength $\{\Omega_j^r\}$. The theoretical plots are obtained by fitting a Jaynes-Cummings-Hubbard model [Hamiltonian in Eqs. (1) and (2)] with free parameters $\{\Omega_j^r\}$, $\{\omega_j\}$, and $\{\kappa_{jk}\}$ using all evolution data sets collectively. Error bars represent statistical uncertainties of 2σ.

this site is suppressed when the energy splitting of the first excited states $|\pm,1\rangle$ is much larger than the hopping rate. This implies that when $|\kappa_{jk}| \ll |\Omega_k^r/2 \pm \omega_{jk}|$, hopping is suppressed from the jth to the kth site, where the tunable blockade strength is set by the red-sideband Rabi frequency Ω_k^r at the blockaded site k. For ions 2 and 3, a higher suppression is observed compared to ions 1 and 2, where the large phonon mode splitting ω_{12} results in some residual hopping despite the applied blockade (see Supplemental Material [23]).

In Fig. 2, we further observe nonzero phonon occupancies at sites prepared in the motional ground state owing to imperfect initial sideband cooling. Based on the nonoscillatory near-zero phonon occupancies of the hopping data [Figs. 2(a), 2(c), and 2(g) for ions 3, 1, and 2, respectively], we estimate average local mode phonon numbers of $\{\bar{n}_1, \bar{n}_2, \bar{n}_3\} = \{0.09, 0.08, 0.04\}$. This also leads to an imperfect preparation and measurement of state $|g,1\rangle$, which additionally suffers from residual phonon hopping over the finite duration of sideband π pulses.

We fit the hopping data to a theoretical model using the Hamiltonian presented in Eqs. (1) and (2), with ω_{jk}, κ_{jk}, and Ω_j^r as free parameters. The steady-state phonon occupancy, in the absence of hopping (see Fig. 3), is used to characterize the systematic errors in the preparation and measurement of the states $|g,0\rangle$ and $|g,1\rangle$. This is subsequently incorporated into all theoretical curves in Fig. 2 [24] (see Supplemental Material [23]). The effect of imperfect sideband cooling is directly included by starting from a thermal phonon distribution with mean phonon numbers $\{\bar{n}_j\}$. Both the spin and the motional degrees of freedom are considered in the theoretical simulation of the full hopping dynamics. A single set of parameters (see Table I) is used to fit all data in Fig. 2, which shows a very good agreement between the experimental data and the theoretical description of the system. The hopping and blockade strengths given by the parameter values of κ_{jk} and Ω_j^r are consistent with those measured directly from the interion distance and red-sideband spectroscopy, respectively [see Supplemental Fig. S1(b) [23]].

A straightforward way to improve fidelities of local phonon operations is to set the sideband Rabi frequency much larger than the hopping strength. In this experiment, since the Raman transition drives both transverse modes, the maximum Rabi frequency is limited by the spacing between the modes $(\omega_x - \omega_y = 2\pi \times 250)$ kHz. In future experiments, this can be resolved by rotating the two principle axes of transverse motion (X and Y) with respect to the Raman beams such that only one mode is excited. For multiphonon hopping experiments, it is also necessary to implement the fast measurement of phonon distributions (instead of single-phonon occupancy) using cascaded sideband pulses, as has been implemented on single ions [27,28].

The stable nonlinearity in the local mode energies is a result of nonuniform rf and dc electric fields in the ion trap. We believe this to be due to an imperfect trap shape and alignment [29]. This can be avoided by using a more linear ion trap, such as a state of the art surface trap, which will

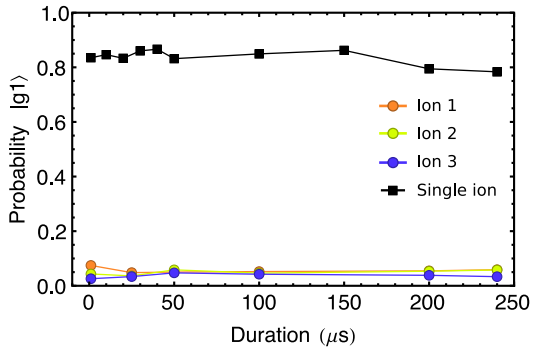

FIG. 3. Steady phonon occupancy observed in the absence of hopping when a single ion is prepared in state $|g,1\rangle$ or in a chain of three ions where each is sideband cooled and prepared in state $|g,0\rangle$. For the single-ion experiment, a constant phonon occupancy indicates negligible cross talk with other transverse and axial modes of the ion trap. In a three-ion chain, the near-zero phonon occupancy indicates that the combined effect of the local mode heating rate and cross talk with other transverse modes (that are not sideband cooled) is negligible. The duration of both experiments is similar to that used to observe the hopping dynamics in Fig. 2. The probabilities of detecting single-phonon excitations in both cases are used to estimate the state preparation and measurement fidelity of states $|g,0\rangle$ and $|g,1\rangle$. Error bars showing statistical uncertainties of 2σ are smaller than experimental data points.

TABLE I. Observed experimental parameters relevant to phonon hopping and blockade in units of $2\pi \times$ kHz, where the local mode energy splitting is ω_{jk} and the hopping rate is κ_{jk} between ions j and k. The values obtained from fits to the hopping data (Fig. 2) are compared with those obtained from direct measurement. The measured hopping rate is obtained from interion distances $\{d_{12}, d_{23}\} = \{10.1(2), 10.0(2)\}$ μm, where the systematic error is due to uncertainty in d_{jk}. The measured red-sideband Rabi frequency Ω_j^r is directly obtained from sideband spectroscopy (see Supplemental Material [23]). The local mode frequencies measured directly from sideband spectroscopy are not shown, as they suffer from large Stark shifts, which are sensitive to variations in the alignment of Raman beams between experimental runs [26].

Parameter	Fitted value	Measured value
ω_{12}	11.58	...
ω_{23}	7.36	...
κ_{12}	2.90	3.27(19)
κ_{23}	2.96	3.36(20)
Ω_1^r	39.7	43.1(16)
Ω_2^r	45.9	47.6(14)
Ω_3^r	46.3	46.0(19)

also allow the system to be scaled to larger ion crystals while maintaining uniform and locally controllable transverse confinement.

Tunable local phonon blockades can be a useful tool in studying energy transport in ion chains [30]. It can also, in principle, be used in mechanically isolating pairs of ions in a crystal for the implementation of fast entangling gates mediated by their local phonon modes [5,31].

This work was supported by the Army Research Office (ARO) with funds from the Intelligence Advanced Research Projects Activity LogiQ program, the Air Force Office of Scientific Research Multidisciplinary University Research Initiative (MURI) program on Quantum Measurement and Verification, the ARO MURI program on Modular Quantum Circuits, and the National Science Foundation Physics Frontier Center at Joint Quantum Institute.

*sdebnath@terpmail.umd.edu

[1] R. Islam, C. Senko, W. C. Campbell, S. Korenblit, J. Smith, A. Lee, E. E. Edwards, C.-C. J. Wang, J. K. Freericks, and C. Monroe, Emergence and frustration of magnetism with variable-range interactions in a quantum simulator, Science **340**, 583 (2013).

[2] T. Monz, D. Nigg, E. A. Martinez, M. F. Brandl, P. Schindler, R. Rines, S. X. Wang, I. L. Chuang, and R. Blatt, Realization of a scalable Shor algorithm, Science **351**, 1068 (2016).

[3] S. Debnath, N. M. Linke, C. Figgatt, K. A. Landsman, K. Wright, and C. Monroe, Demonstration of a small programmable quantum computer with atomic qubits, Nature (London) **536**, 63 (2016).

[4] S.-L. Zhu, C. Monroe, and L.-M. Duan, Trapped Ion Quantum Computation with Transverse Phonon Modes, Phys. Rev. Lett. **97**, 050505 (2006).

[5] S. L. Zhu, C. Monroe, and L. M. Duan, Arbitrary-speed quantum gates within large ion crystals through minimum control of laser beams, Europhys. Lett. **73**, 485 (2006).

[6] D. Porras and J. I. Cirac, Bose-Einstein Condensation and Strong-Correlation Behavior of Phonons in Ion Traps, Phys. Rev. Lett. **93**, 263602 (2004).

[7] P. A. Ivanov, S. S. Ivanov, N. V. Vitanov, A. Mering, M. Fleischhauer, and K. Singer, Simulation of a quantum phase transition of polaritons with trapped ions, Phys. Rev. A **80**, 060301 (2009).

[8] A. Mering, M. Fleischhauer, P. A. Ivanov, and K. Singer, Analytic approximations to the phase diagram of the Jaynes-Cummings-Hubbard model, Phys. Rev. A **80**, 053821 (2009).

[9] K. Toyoda, R. Hiji, A. Noguchi, and S. Urabe, Hong-Ou-Mandel interference of two phonons in trapped ions, Nature (London) **527**, 74 (2015).

[10] C. Shen, Z. Zhang, and L.-M. Duan, Scalable Implementation of Boson Sampling with Trapped Ions, Phys. Rev. Lett. **112**, 050504 (2014).

[11] D. Leibfried, R. Blatt, C. Monroe, and D. Wineland, Quantum dynamics of single trapped ions, Rev. Mod. Phys. **75**, 281 (2003).

[12] A. D. Greentree, C. Tahan, J. H. Cole, and L. C. L. Hollenberg, Quantum phase transitions of light, Nat. Phys. **2**, 856 (2006).

[13] M. J. Hartmann, F. G. S. L. Brandão, and M. B. Plenio, Strongly interacting polaritons in coupled arrays of cavities, Nat. Phys. **2**, 849 (2006).

[14] K. Toyoda, Y. Matsuno, A. Noguchi, S. Haze, and S. Urabe, Experimental Realization of a Quantum Phase Transition of Polaritonic Excitations, Phys. Rev. Lett. **111**, 160501 (2013).

[15] K. R. Brown, C. Ospelkaus, Y. Colombe, A. C. Wilson, D. Leibfried, and D. J. Wineland, Coupled quantized mechanical oscillators, Nature (London) **471**, 196 (2011).

[16] M. Harlander, R. Lechner, M. Brownnutt, R. Blatt, and W. Hänsel, Trapped-ion antennae for the transmission of quantum information, Nature (London) **471**, 200 (2011).

[17] S. Haze, Y. Tateishi, A. Noguchi, K. Toyoda, and S. Urabe, Observation of phonon hopping in radial vibrational modes of trapped ions, Phys. Rev. A **85**, 031401 (2012).

[18] C. Hamsen, K. N. Tolazzi, T. Wilk, and G. Rempe, Two-Photon Blockade in an Atom-Driven Cavity QED System, Phys. Rev. Lett. **118**, 133604 (2017).

[19] S. Olmschenk, K. C. Younge, D. L. Moehring, D. N. Matsukevich, P. Maunz, and C. Monroe, Manipulation and detection of a trapped Yb+ hyperfine qubit S, Phys. Rev. A **76**, 052314 (2007).

[20] D. Hayes, D. N. Matsukevich, P. Maunz, D. Hucul, Q. Quraishi, S. Olmschenk, W. Campbell, J. Mizrahi, C. Senko, and C. Monroe, Entanglement of Atomic Qubits Using an Optical Frequency Comb, Phys. Rev. Lett. **104**, 140501 (2010).

[21] Model H-601 Series 32-Channel UV Acousto-Optic Modulator, PN: 66948-226460-G01, Harris Corporation.

[22] Model WX1284C-1 1.25 GS/s Four Channel Arbitrary Waveform Generator, PN: 126182, Tabor Electronics Ltd.

[23] See Supplemental Material at http://link.aps.org/supplemental/10.1103/PhysRevLett.120.073001 for methods and additional explanation of hopping and blockade data, which includes Refs. [24,25].

[24] C. Shen and L.-M. Duan, Correcting detection errors in quantum state engineering through data processing, New J. Phys. **14**, 053053 (2012).

[25] K. G. Johnson, J. D. Wong-Campos, A. Restelli, K. A. Landsman, B. Neyenhuis, J. Mizrahi, and C. Monroe, Active stabilization of ion trap radiofrequency potentials, Rev. Sci. Instrum. **87**, 053110 (2016).

[26] A. C. Lee, J. Smith, P. Richerme, B. Neyenhuis, P. W. Hess, J. Zhang, and C. Monroe, Engineering large Stark shifts for control of individual clock state qubits, Phys. Rev. A **94**, 042308 (2016).

[27] S. An, J.-N. Zhang, M. Um, D. Lv, Y. Lu, J. Zhang, Z.-Q. Yin, H. T. Quan, and K. Kim, Experimental test of the quantum Jarzynski equality with a trapped-ion system, Nat. Phys. **11**, 193 (2015).

[28] M. Um, J. Zhang, D. Lv, Y. Lu, S. An, J.-N. Zhang, H. Nha, M. S. Kim, and K. Kim, Phonon arithmetic in a trapped ion system, Nat. Commun. **7**, 11410 (2016).

[29] S. Debnath, Ph.D. thesis, University of Maryland, College Park, 2016, https://drum.lib.umd.edu/handle/1903/18990.

[30] M. Ramm, T. Pruttivarasin, and H. Häffner, Energy transport in trapped ion chains, New J. Phys. **16**, 063062 (2014).

[31] J. D. Wong-Campos, S. A. Moses, K. G. Johnson, and C. Monroe, Demonstration of Two-Atom Entanglement with Ultrafast Optical Pulses, Phys. Rev. Lett. **119**, 230501 (2017).